



Apelin-13 attenuates early brain injury through inhibiting inflammation and apoptosis in rats after experimental subarachnoid hemorrhage

Xiaoyan Shen^{1,2} · Guiqiang Yuan¹ · Bing Li^{1,3} · Cheng Cao^{1,4} · Demao Cao^{1,5} · Jiang Wu¹ · Xiang Li¹ · Haiying Li¹ · Haitao Shen¹ · Zhong Wang¹ · Gang Chen¹

Received: 30 December 2020 / Accepted: 26 November 2021 / Published online: 9 January 2022
© The Author(s), under exclusive licence to Springer Nature B.V. 2022

Abstract

Background Early brain injury (EBI) has been considered as the major contributor to the neurological dysfunction and poor clinical outcomes of subarachnoid hemorrhage (SAH). Studies showed that apelin-13 exhibits a neuroprotective effect in brain damage induced by cerebral ischemia. However, it remains unclear whether apelin-13 could exhibit the protective functions following SAH. The present study aimed to validate the neuroprotective role of apelin-13 in SAH, and further investigated the underlying mechanisms.

Methods and results We constructed SAH rat model and we found that apelin-13 significantly alleviated neurological disorder and brain edema, improved memory deficits in SAH rats. Apelin-13 treatment decreased contents of TNF- α and IL-1 β in cerebral spinal fluid of SAH rat by using ELISA. Apelin-13 treatment promoted the expression of APJ and Bcl-2, and decreased the level of active caspase-3 and Bax in the temporal cortex after SAH by using western blot. Also, apelin-13 attenuated the cortical cell death and neuronal degeneration as shown by TUNEL, FJB and Nissl staining. However, ML221, an inhibitor of APJ, significantly reversed all the above neuroprotective effects of apelin-13. Moreover, a neuron-microglia co-culture system, which mimic SAH in vitro, confirmed the protective effect of apelin-13 on neurons and the inhibitory effect on inflammation through apoptosis-related proteins.

Conclusions These data demonstrated that apelin-13 exhibit a neuroprotective role after SAH through inhibition of apoptosis in an APJ dependent manner.

Keywords Apelin-13 · APJ · Inflammation · Apoptosis · Subarachnoid hemorrhage

Abbreviations

ANOVA	Analysis of variance
APJ	G protein-coupled receptor-apelin and angiotensin-1-like receptor
Bax	Bcl-2 associated x protein
Bcl-2	B-cell lymphoma 2

Xiaoyan Shen and Guiqiang Yuan have contributed equally to this work.

✉ Haitao Shen
shenhaitao1990@suda.edu.cn

✉ Zhong Wang
wangzhong8761@163.com

¹ Department of Neurosurgery & Brain and Nerve Research Laboratory, The First Affiliated Hospital of Soochow University, 188 Shizi Street, Suzhou 215006, Jiangsu Province, China

² Department of Neurosurgery, Renji Hospital, Shanghai Jiao Tong University School of Medicine, No. 160, Pujian Road, Pudong District, Shanghai 200127, China

³ Department of Neurosurgery, Yancheng City No. 1 People's Hospital, The Fourth Affiliated Hospital of Nantong University, Yancheng, Jiangsu Province, China

⁴ Department of Neurocritical Intensive Care Unit, The Affiliated Jiangyin Hospital, School of Medicine, Southeast University, Jiangyin, Jiangsu Province, China

⁵ Department of Neurosurgery, The Affiliated Hospital of Yangzhou University, Yangzhou, Jiangsu Province, China

CSF	Cerebral spinal fluid
DAPI	4',6-Diamidino-2-phenylindole
DMSO	Dimethylsulfoxide
dUTP	2'-Deoxyuridine 5'-Triphosphate
EBI	Early brain injury
ER	Endoplasmic reticulum
FJB	Fluoro-Jade B
GLP-1R/PI3K/Akt	Glucagon-like peptide-1/phosphatidylinositol 3-kinase/protein kinase B
IL-1 β	Interleukin-1 β
PBS	Phosphate buffer solution
ML221	4-Oxo-6-((pyrimidin-2-ylthio)methyl)-4H-pyran-3-yl 4-nitrobenzoate
MWM	Morris water maze
Nrf2	Nuclear factor erythroid 2-related factor-2
ROS	Reactive oxygen species
SAH	Subarachnoid hemorrhage
SD	Sprague–Dawley
TNF- α	Tumor necrosis factor- α
WW/DW	Wet weight/dry weight
Means \pm SD	Means \pm standard deviation
IF	Immunofluorescence
MTT	3-(4,5-Dimethylthiazol-2-yl)-2,5-diphenyltetrazolium bromide

Introduction

Subarachnoid hemorrhage (SAH) is reported to be related with elevated rates of mortality and morbidity, which accounts for about 5% of all stroke cases [1]. Rupture of a cerebral aneurysm which located at the skull base is the most common cause in 85% spontaneous SAH cases [2]. Despite significant improvements attributed to the microsurgical aneurysm clipping and endovascular interventional therapy, the outcome of SAH is still dissatisfactory. Effects are limited to overcome brain damage and improve the ending of SAH, especially the poor-grade ones [3]. Following SAH, previous literature has reported the occurrence of early brain injury (EBI) and cognitive deficits. EBI has been regarded as the major contributor to the neurological dysfunction and poor clinical outcomes in patients following SAH [4, 5]. Thus, therapeutic inhibition of EBI may represent a novel and promising approach in the management of SAH cases. However, the precise underlying mechanism of the pathogenesis of EBI remains obscure, greatly impeding the development of effective therapeutic modality for EBI [6, 7]. Therefore, elucidating the underlying molecular mechanism of EBI is critical for develop novel and effective therapeutic approach against SAH.

Apelin is a ligand of G protein-coupled receptor-apelin and angiotensin-1-like receptor (APJ). After translocation, apelin cleavages into four different peptide components, such as apelin-17, apelin-36, apelin-12, and apelin-13. Of note, apelin-13 is one of the most active form of apelin, possessing the highest plasma concentration and greatest biological activity [8]. Accumulating evidences demonstrated that apelin-13 functions as a protective factor against brain injury. Apelin-13 could decrease brain water content, inhibit cell apoptosis, and improve motor function in an animal model following intracerebral hemorrhage [9]. Moreover, apelin-13 exhibits neuroprotective roles in brain ischemic/reperfusion injury induced by reactive oxygen species (ROS)-mediated oxidative stress and inflammatory response; mechanically, apelin-13 activates AMPK/GSK-3 β pathway and further enhances the expression of Nrf2-regulated antioxidant enzymes [10]. Taken together, apelin-13 may represent a potential target for therapeutic intervention in brain injury. However, the protective effect of apelin-13/APJ system in SAH remains not fully elucidated.

In this research, we evaluated the effects of apelin-13 on neurological impairment, brain edema, neuroinflammation and spatial memory deficits in a rat SAH model. In addition, apelin-13 was administrated intracerebroventricularly in SAH model of rats and the neuronal apoptosis and degeneration were evaluated. Moreover, an APJ antagonist, ML221 (4-oxo-6-((pyrimidin-2-ylthio)methyl)-4H-pyran-3-yl 4-nitrobenzoate), was used to furthermore investigate the neuroprotective efficacy of apelin-13/APJ signaling following SAH. Finally, the neuroprotective effect of apelin-13/APJ signaling was verified in vitro SAH model.

Materials and methods

Ethics and animals

Animals were purchased from the Animal Center of Soochow University (Suzhou, China). These adult male Sprague–Dawley (SD) rats weighing 280 g to 320 g were housed under a 12:12 h light–dark cycle and a temperature of 23 ± 1 °C and humidity of 40%. Food and water were provided ad libitum. We used these animals and abided by the guidelines of the National Institutes of Health. Manipulation of animals were approved by the Institutional Animal Care Committee of Soochow University.

Animal study design and drug administration

This animal study was divided into two parts: experiment 1 and experiment 2, and the experimental design was shown in Fig. 1. All rats were numbered and divided into several groups using a table of random numbers by a technician who

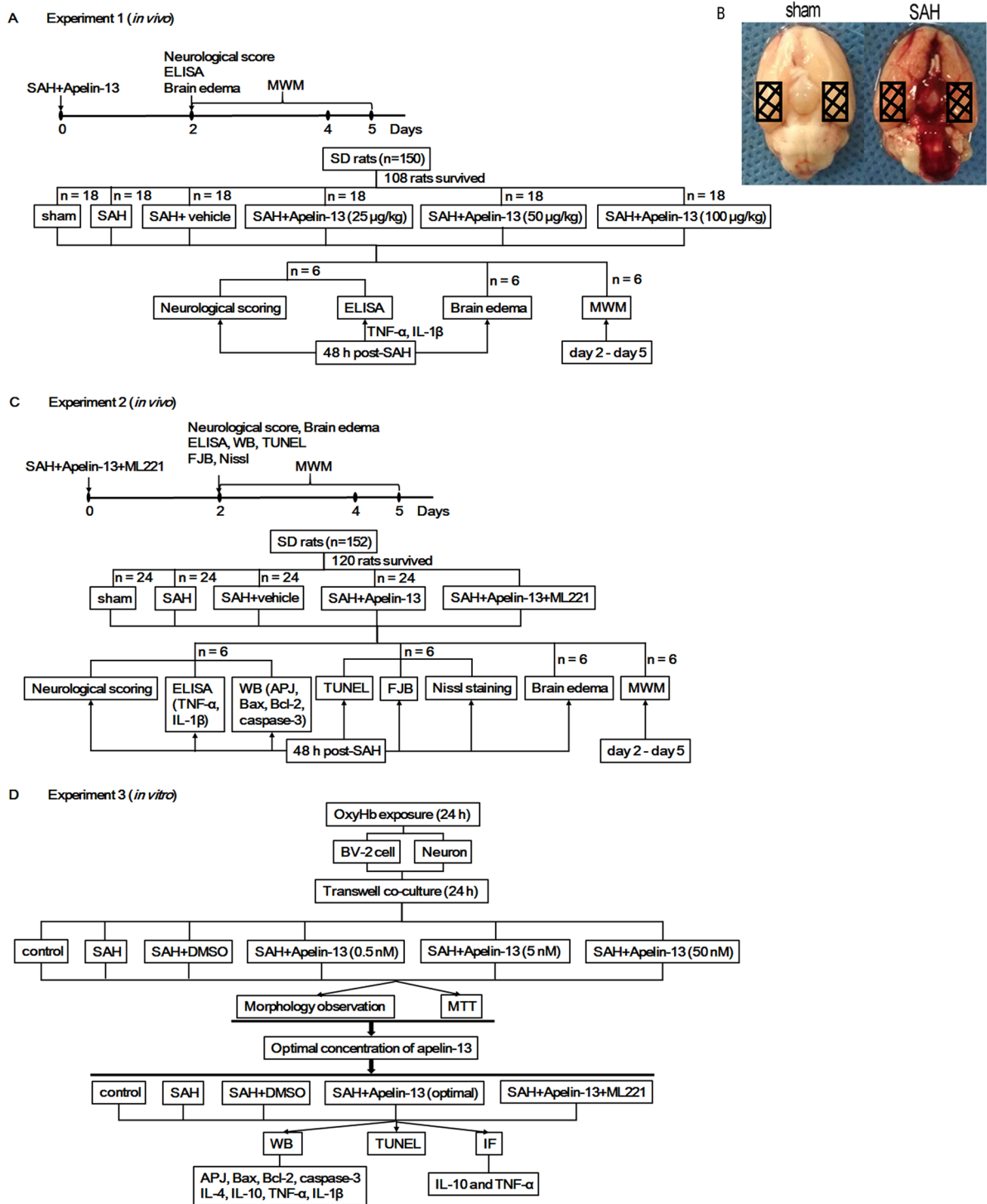


Fig. 1 Establishment of SAH model in rats and study design. **A** In the Experiment 1, the timeline and groups. A total of 150 male SD rats were used and 108 rats were survived, which were then randomly divided to 6 groups ($n=18$): sham group, SAH group, SAH+vehicle (saline) group, SAH+apelin-13 at 25 µg/kg, 50 µg/kg or 100 µg/kg groups. **B** Schematic representation of the sham group and the SAH group, the dash area on the temporal cortex showed brain tissues used for western blot analysis. **C** In the Experiment 2, the timeline and groups. A total of 152 male SD rats were used and 120 survived

rats were randomly divided into 5 groups ($n=24$): sham group, SAH group, SAH+vehicle (DMSO) group, SAH+apelin-13 (50 µg/kg) group, and SAH+apelin-13+ML221 group. **D** In the Experiment 3, to mimic SAH in vitro, neurons and BV-2 cells were induced with 25 µM OxyHb alone for 24 h and then transferred to the Transwell co-culture system to screen for optimal concentration of apelin-13. The co-culture system of BV-2 and neurons remained unchanged and added the optimal concentration of apelin-13 and then divided into 5 groups: control, SAH, SAH+DMSO, SAH+apelin-13, SAH+apelin-13+ML221

was entirely blind to this study. In behavioral impairment, brain edema, ELISA and Morris water maze (MWM) test, the technician was entirely blind to this experimental groups.

In the experiment 1 (Fig. 1A), a total of 150 SD rats was prepared while 108 rats survived (18 rats come from the Sham group, and 90 rats surviving after surgery from an initial 132 rats in the SAH group). Survival rats were randomly classified into six groups (18 rats per group): Sham group; SAH; SAH + vehicle (saline); SAH + apelin-13 (25 µg/kg); SAH + apelin-13 (50 µg/kg); and SAH + apelin-13 (100 µg/kg).

For SAH group: to establish a rat model of SAH [11], animals were anesthetized following intraperitoneal injection of 4% chloral hydrate at a dosage of 1 mL/100 g. Then, the rat lay prostrate with its head located in a suitable position by fixing firmly in a stereotaxic apparatus (Zhenghua Biologics, Anhui, China). The bregma was exposed through a middle scalp incision. With the site of 7.5 mm anterior to the bregma, a miniature drilling was used to create a 1 mm hole. The needle was placed at an angle of 45° from the sagittal plane, inserted slowly towards the midline. The needle was advanced 11 mm into the prechiasmatic cistern and reached the depth about 2–3 mm anterior to the chiasm, and retracted 0.5 mm. Then, 300 µL of fresh and non-heparinized blood extracted from left inguinal artery were injected into prechiasmatic cistern in 20 s.

For sham group: All the procedures of surgery were same as the SAH group. But, the rat in the sham group underwent administration 300 µL saline rather than fresh and non-heparinized blood.

For SAH + apelin-13 group: All the procedures of surgery were same as the SAH group. Rats were administered apelin-13 immediately after SAH induction. Rats were injected intracerebroventricularly with apelin-13 (ab141010, Abcam, USA) at 25 µg/kg, 50 µg/kg, and 100 µg/kg, by using a Hamilton microsyringe. The dosage of apelin-13 was chosen according to the previous article described with minor modifications [12]. The hole for drug injection located lateral 1.5 mm from the bregma and depth 3.5 mm from the skull bone. The Hamilton microsyringe was stayed for 5 min in order to let the drugs dilute into the ventricle maximally.

For SAH + vehicle group: All the procedures were same as the SAH + apelin-13 group. But, the drugs of apelin-13 was replaced by 10 µL physiological saline.

After surgery, the incision was then sutured and 5 mL of 0.9% NaCl was injected subcutaneously to prevent dehydration of experimental rats. All animals were placed appropriately and recover for 45 min. After recovery, animals were put back to their individual cages and food and water were provided without restriction. The feeding room was maintained with suitable humidity and was kept at the temperature of 23 ± 1 °C. The inferior basal temporal lobe was stained with blood if the SAH model was

established correctly (Fig. 1B). To satisfy all groups have equal numbers, new rats were included in the study to substitute dead.

In the experiment 2 (Fig. 1C), a total of 152 SD rats was prepared while 120 rats survived (24 rats come from the Sham group, and 96 rats surviving after surgery from an initial 128 rats in the SAH group). Survival rats were randomly classified into five groups (24 rats per group): Sham group; SAH group; SAH + vehicle (DMSO); SAH + apelin-13 (50 µg/kg); and SAH + apelin-13 + ML221.

For Sham group, SAH group, and SAH + apelin-13 (50 µg/kg) group: All surgical procedures were the same as the description above in the experiment 1. The dosage of 50 µg/kg of apelin-13 was chosen from Experiment 1 according to the results.

For SAH + apelin-13 + ML221 group: All surgical procedures were the same as the SAH + apelin-13 (50 µg/kg) group, while the difference was that after injecting apelin-13, 50 µg/kg ML221 (SML0919, Sigma, USA) [13] was injected immediately in the same bone hole. In this process, after injecting apelin-13, the needle was retracted slowly and irrigated with physiological saline three times, and then the needle was reinserted on a stereotaxic apparatus to ensure the ML221 was injected from the same bone hole.

For SAH + vehicle group: All surgical procedures were the same as the SAH + apelin-13 group, while the apelin-13 was replaced by DMSO.

Postoperative management of each group was the same as in experiment 1.

Sample collection

Animals were sacrificed at the time point of 48 h post-SAH-modeling except those for MWM test. The MWM experiment began on the second day after SAH modeling and was performed for 4 consecutive days. Neurological score and brain edema were assessed 48 h after modeling of SAH. For ELISA, the cerebral spinal fluid (CSF) samples were collected by puncturing the cisterna magna, the neck skin was cut open with a straight incision and the muscles were exposed, an injection syringe was slowly inserted towards the cisterna magna, as described previously [14]. Approximately 100 µL CSF were extracted and centrifuged immediately and retained supernatant for ELISA detections. The bilateral temporal base brain tissues near to the blood clots (about 100 mg/each rat) (Fig. 1B) were collected for western blotting. The total coronal sections containing temporal base brain tissues (Fig. 1B) were applied to TUNEL, FJB and Nissl staining. In every figure, the “n” represented the sample size.

Cell culture and stimulation

The primary cortical neurons of rats was purchased from Procell (CP-R105, China) and cultured in complete culture medium of rat cortical neurons (Procell, CM-R105). The primary microglia of BV-2 cells were purchased from Procell (CL-0493, China) and cultured in Minimum Essential Medium (Procell, PM150410), which supplemented 10% fetal bovine serum and 1% penicillin–streptomycin. Neuron and BV-2 cells were placed in an incubator at 37 °C with 5% CO₂. To mimic SAH in vitro (Fig. 1D), neurons and BV-2 cells were induced with 25 μM oxyhemoglobin (OxyHb) alone for 24 h and then transferred to the Transwell co-culture system [15]. The different concentrations of apelin-13 (0.5 nM, 5 nM, 50 nM) was respectively added into co-culture Transwell system and cultured for another 24 h. After co-culture, the morphology of neurons and BV-2 cell were observed and the number was detected by MTT.

According to the results of cell morphology observation and MTT, the optimal concentration of apelin-13 was selected for subsequent experiments. The co-culture system of BV-2 and neurons remained unchanged and was divided into 5 groups: control, SAH, SAH + DMSO, SAH + apelin-13, SAH + apelin-13 + ML221. For control group, BV-2 and neurons were co-cultured in Transwell system but were not pretreated with OxyHb exposure. For SAH group, neurons and BV-2 cells were induced with OxyHb alone for 24 h and then transferred to the Transwell co-culture system. For SAH + apelin-13 group, after SAH induction, the optimal concentration of apelin-13 was added and the culture continued for 24 h. For SAH + DMSO group, all the procedures were the same as for group SAH + apelin-13, except that apelin-13 was replaced by 10% DMSO. For SAH + apelin-13 + ML221 group, all the procedures were the same as for group SAH + apelin-13, but ML221 was added immediately after apelin-13. After culture, neuronal apoptosis was detected by using TUNEL staining, and the expression of apoptosis-related proteins (Bcl2, Bax, and active caspase-3), and inflammatory factors (IL-4, IL-10, TNF-α, and IL-1β) of BV-2 were detected by using western blotting or immunofluorescence (IF).

Statistical analysis

Our data were illustrated as means ± standard deviation (means ± SD) and subject to statistical analysis by GraphPad Prism 6.0. First, we assessed the normality and homoscedasticity of the data. Then, when the data was satisfied normality and homogeneity of variance, continuous variables was compared by one-way analysis of variance (ANOVA) followed by Tukey's test. Next, data that did not satisfy normality and homogeneity of variance were subjected for nonparametric test, and the Mann–Whitney U-test and

kruskal–wallis were used to compare the changes of neurological scores and MWM, respectively. Differences between two groups were compared by t tests. A probability of value of $P < 0.05$ was considered to be statistically significant.

The other materials and methods used in this study are described in the Supplemental Material.

Results

General observations and mortality rate of rats following SAH

In our experiment, data regarding body weight, body temperature, arterial blood gas, and mean arterial blood pressure were measured, and no significant differences between each experimental group were observed (data not shown). No rats died in the sham group both in the experiment 1 and 2. The mortality rate of SAH rats was 28% (42/150) in experiment 1 and 21% (32/152) in experiment 2, and then survival rats were used for following experiment and no died until end. The detail mortality for each group is shown in Supplemental Table 1. As shown in Fig. 1B, blood clots were located at the surface of brainstem and Willis cycle, suggesting the successful establishment of SAH model in rats.

Apelin-13 alleviated neurological deficits and brain edema, improved spatial memory, and inhibited inflammation in SAH rats

First, we accessed the effect of apelin-13 at three concentration on neurological score and brain edema in SAH rats. Compared to the rats in the sham group, neurological scores and brain edema were elevated in SAH rats. Administration of apelin-13 at 25 μg/kg had no significant effects on neurological score but significantly reduced brain edema. However, the neurological scores and brain edema in apelin-13 at 50 μg/kg and 100 μg/kg groups were significantly lower than vehicle group ($P < 0.05$, Fig. 2A, B). Next, we evaluated the role of apelin-13 on the spatial memory of SAH rats using MWM test. As a result, swimming distance and escape latency trends were similar to the neurological score in each group, apelin-13 at 50 μg/kg and 100 μg/kg showed significant reduction (Fig. 2C–E). Finally, we accessed the regulatory role of apelin-13 on pro-inflammatory cytokine in SAH rats. The levels of IL-1β and TNF-α were increased after SAH induction, and apelin-13 at three concentration were suppressed the levels of IL-1β and TNF-α in CSF samples, compared to the rats in the vehicle group (Fig. 2F, G). Moreover, the levels of IL-1β and TNF-α showed no difference between apelin-13 at 100 μg/kg and 50 μg/kg ($P > 0.05$, Fig. 2F, G). Taken together, apelin-13 could alleviate the neurological deficit and brain edema, improve

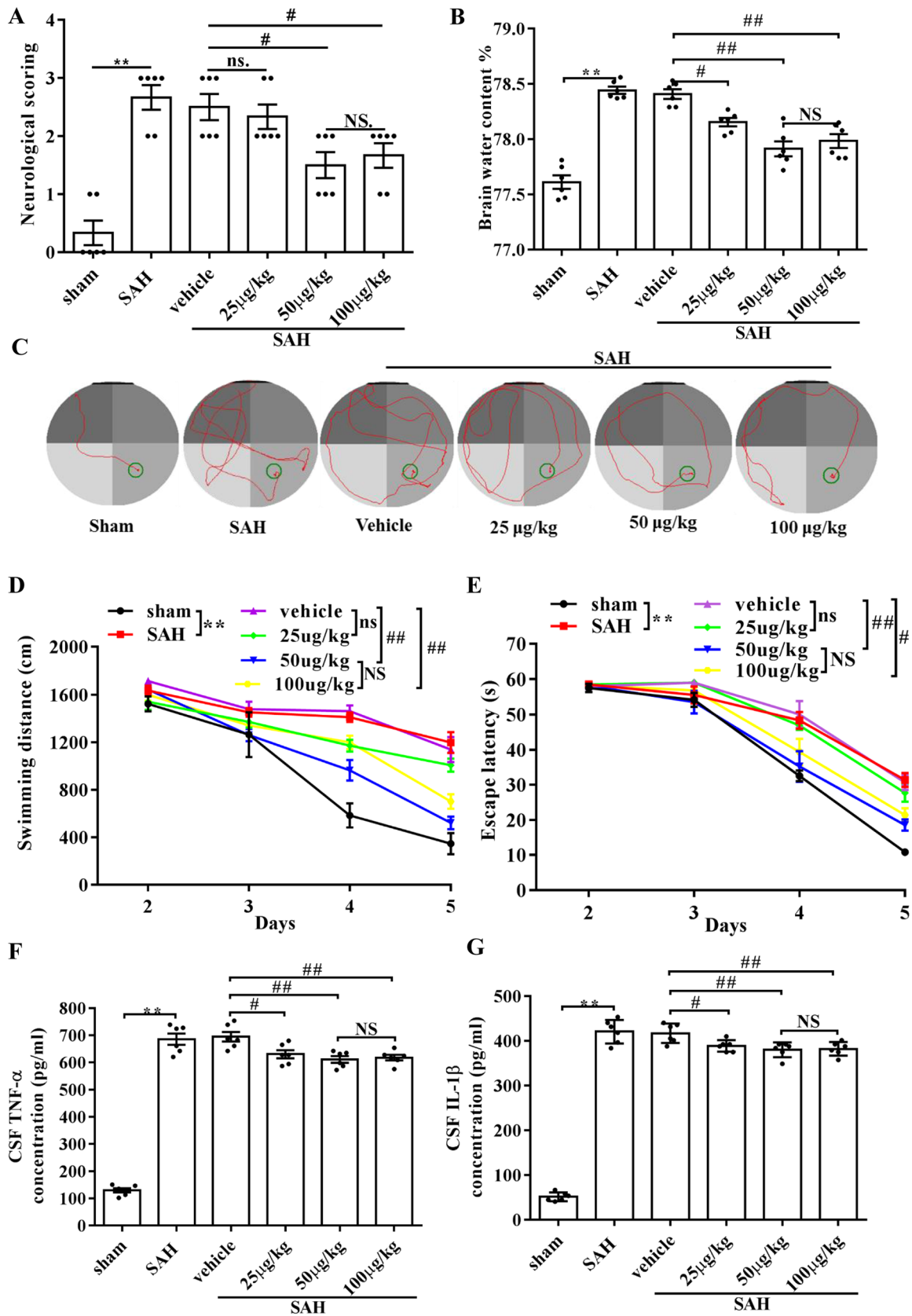


Fig. 2 Apelin-13 alleviated neurological deficits, reduced brain edema, promoted spatial memory, and inhibited inflammation after SAH. **A** Compared to the sham group, SAH rats showed higher neurological scores. Apelin-13 at 50 $\mu\text{g}/\text{kg}$ and 100 $\mu\text{g}/\text{kg}$ decreased neurological scores. **B** The brain edema was determined by the percentage of brain water content. Apelin-13 treatment reduced cerebral edema induced by SAH. **C** The locus diagram of MWM. The swimming distance (**D**) and escape latency (**E**) in SAH rats treated with or without apelin-13. The TNF- α (**F**) and IL-1 β (**G**) in CSF contents in SAH rats treated with or without apelin-13. All data were expressed as mean \pm SD ($n=6$, each group). $^{**}P<0.01$ vs sham group, $^{\#}P<0.05$ and $^{\#\#}P<0.01$ vs SAH + vehicle group, $^{\text{ns}}P>0.05$ vs SAH + vehicle group, $^{\text{NS}}P>0.05$ vs SAH + apelin-13 50 $\mu\text{g}/\text{kg}$ group

spatial memory and inhibit inflammatory response in SAH rats, and apelin-13 at the dosage of 50 $\mu\text{g}/\text{kg}$ exhibited the most beneficial neuroprotective effect.

Apelin-13 alleviated brain injury depending on APJ in SAH rats

Given the results in Fig. 2, 50 $\mu\text{g}/\text{kg}$ of apelin-13 was selected for subsequent rat experiments. As expected, 50 $\mu\text{g}/\text{kg}$ of apelin-13 treatment reduced neurological scores and brain edema, improved spatial memory and inhibited the level of IL-1 β and TNF- α in SAH rats (Fig. 3A–G). However, administration with ML221, an inhibitor of APJ, significantly weakened the above neuroprotective role of apelin-13 in SAH rats (Fig. 3A–G). Besides, the expression of APJ was significantly increased in SAH rats, and apelin-13 treatment further elevated APJ expression, but ML221 attenuated the expression of APJ and blocked the effect of apelin-13 (Fig. 4A). These results suggested that apelin-13 alleviated brain injury depended on APJ. Study reported that apelin protect dopaminergic neuron through APJ and apoptosis pathway [16]. Thus, we next investigated the effect of apelin-13/APJ on the expression of apoptosis-related proteins. As a result, the protein levels of Bax and active caspase 3 were significantly elevated while the Bcl-2 was reduced after SAH induction, compared to the sham group ($P<0.01$, Fig. 4A). Apelin-13 suppressed the expression levels of Bax and active caspase 3, but increased Bcl-2 expression in SAH rats, which suggesting apelin-13 has a protective against apoptosis in SAH rats ($P<0.01$, Fig. 4A). Whereas, ML221 significantly weakened the apoptosis inhibition of apelin-13 in SAH rats ($P<0.05$, Fig. 4A). The results of TUNEL

staining also showed that apelin-13 significantly reduced the proportion of apoptotic cells, but ML221 abolished this effect (Fig. 4B). Therefore, apelin-13 inhibited neuronal apoptosis, which is dependent on APJ. Consistently, the results of FJB and Nissl staining once again confirmed the protective role of apelin-13/APJ system on neuron in SAH rats (Fig. 4C, D). Taken together, these findings evidenced that apelin-13 alleviated brain injury depending on APJ in SAH rats.

Apelin-13 inhibited apoptosis and inflammation in an APJ-dependent manner after SAH in vitro

To further explore the mechanism of the neuroprotective effect of apelin/APJ system, we investigated the effects of apelin/APJ system on apoptosis-related proteins and inflammatory cytokine in vitro. As shown in Supplemental Fig. 1, in neuron-microglia co-culture system, neurons showed evident neuronal degeneration characterized by swollen bodies with loss of synapses, but apelin-13 administration significantly prevented these morphological changes. Besides, compared with SAH + DMSO group, apelin-13 treatment significantly elevated the viability of neuron cells and the effect was most significant at 5 nM (Supplemental Fig. 2). Thus, 5 nM apelin-13 was used for subsequent cell experiments.

Moreover, OxyHb exposure led to a significant increase in APJ protein expression, and treatment with apelin-13 further enhanced APJ expression, but ML221 blocked this effect of apelin-13 on APJ (Fig. 5A). As expected, OxyHb exposure activated the apoptotic pathways in neurons, showed as an increase expression of Bax and Caspase-3, and decrease Bcl-2 expression (Fig. 5A). Apelin-13 treatment rescued the damage of OxyHb to neurons, while ML221 significantly prevented the inhibitory effect of apelin-13 on apoptosis (Fig. 5A). TUNEL results supported that apelin-13 protect neuron in an APJ dependent manner (Fig. 5B). In addition, the results of western blot and IF showed that, apelin-13 promoted the levels of anti-inflammatory cotykins (IL-4 and IL-10) and inhibited the levels of pro-inflammatory cotykins (IL-1 β and TNF- α) in BV-2 cells, suggesting that apelin-13 regulated inflammatory pathways after SAH in neuron (Fig. 5C, D). The ML221 also could block the effect of apelin-13 on inflammation regulation (Fig. 5C, D). Collectively, apelin-13 inhibited apoptosis and inflammation in an APJ-dependent manner after SAH in vitro.

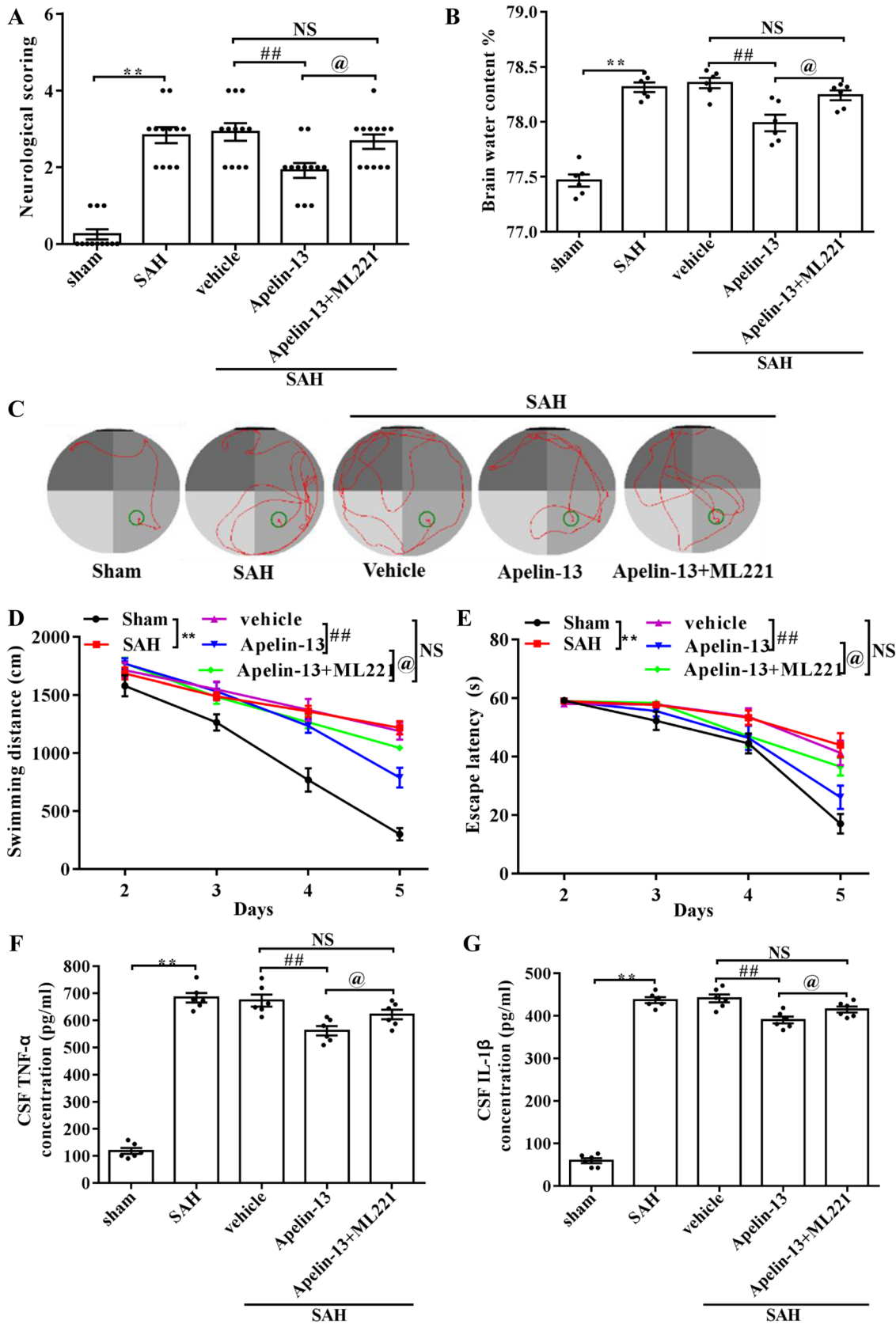


Fig. 3 Apelin-13 reduced neural apoptosis after SAH dependent on APJ. **A** Apelin-13 decreased the neurological scoring. **B** Apelin-13 reduced the brain edema. **C–E** Apelin-13 decreased the swimming distance and latency time in MWM. **F–G** Apelin-13 suppressed the levels of TNF- α and IL-1 β in CSF. All data were represented as mean \pm SD ($n=6$, each group). ** $P < 0.01$ vs sham group, ### $P < 0.01$ vs SAH+vehicle group, @ $P < 0.05$ vs SAH+apelin-13 group, ^{ns} $P > 0.05$ vs SAH+vehicle group

Discussion

Just like a cell signal system, apelin binding APJ to active second messenger signaling cascades [17]. However, up to now, the relationship between apelin/APJ system and SAH has not been clarified clearly. In our study, we demonstrated that apelin-13 exhibit a neuroprotective role through alleviating neurological deficits, promoting spatial memory, and inhibiting inflammation in SAH rats, thereby improve EBI. Mechanically, apelin-13 inhibited apoptosis signal and inflammatory cytokine (TNF- α and IL-1 β) in an APJ dependent manner (Fig. 5E).

Xu et al. found that apelin-13 could alleviate the EBI following SAH by suppressing ER stress-mediated apoptosis

possibly involving Activating transcription factor 6/CCAAT/enhancer-binding protein homologous protein (ATF6/CHOP) pathway [18]. Another study by Liu et al. revealed that the neuroprotective role of apelin-13 is mediated by GLP-1R/PI3K/Akt pathway [19]. However, those studies had some limitations and did not fully reveal the mechanisms involved in EBI and they also did not evaluate the relationship between APJ and apelin-13. Whereas, the apelin-13/APJ system is important in the whole pathological process and effects the outcome of SAH. The data from Xu et al. also indicated apelin-13 binding to APJ can attenuate early brain injury by reducing ER stress-mediated oxidative stress and neuroinflammation [20]. In our experiment, to further evidence the role of the apelin-13/APJ system in SAH-induced EBI, ML221, an inhibitor of APJ, was applied in combination apelin-13. As a result, the apelin-13 remarkably accelerated the expression of APJ while ML221 (an inhibitor of APJ) blocked this effect, which precisely illustrated the dependence between apelin-13 and APJ. Thus, we concluded that apelin-13 protect against brain damage after SAH in an APJ dependent manner. It is worth mentioning that the antagonistic effect of ML221 on APJ appears to be an apelin-dependent. For example, Roche et al. reported

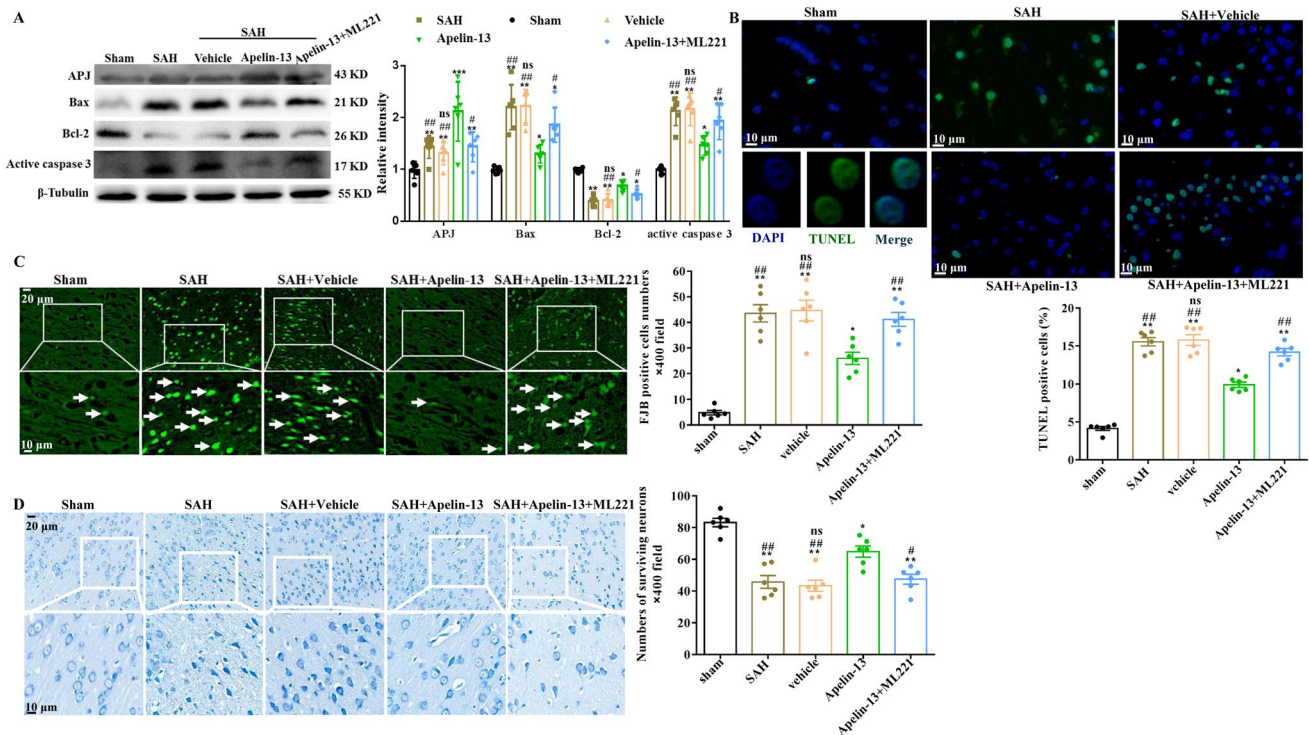


Fig. 4 Apelin-13 protects against cell apoptosis and neural degeneration after SAH in an APJ dependent manner. **A** Western blot indicated the protein levels of APJ, Bax, Bcl-2, and active caspase 3 in each group. **B** Detection of apoptosis by TUNEL staining. Scale bar was 10 μ m. Percentages of TUNEL-positive cells was also indicated. **C** FJB staining showed neuronal degeneration in the cortex of rats in

different groups. Scale bar was 20 μ m for upper and 10 μ m for down. **D** Nissl staining in the temporal cortex of rats. Quantification analysis of the number of viable neurons in temporal cortex. Scale bar was 20 μ m for upper and 10 μ m for down. All data were described as mean \pm SD ($n=6$, each group). *Mean $P < 0.05$ vs sham, #Mean $P < 0.05$ vs Apelin-13, ^{ns}Mean $P > 0.05$ vs SAH. **###Mean $P < 0.01$

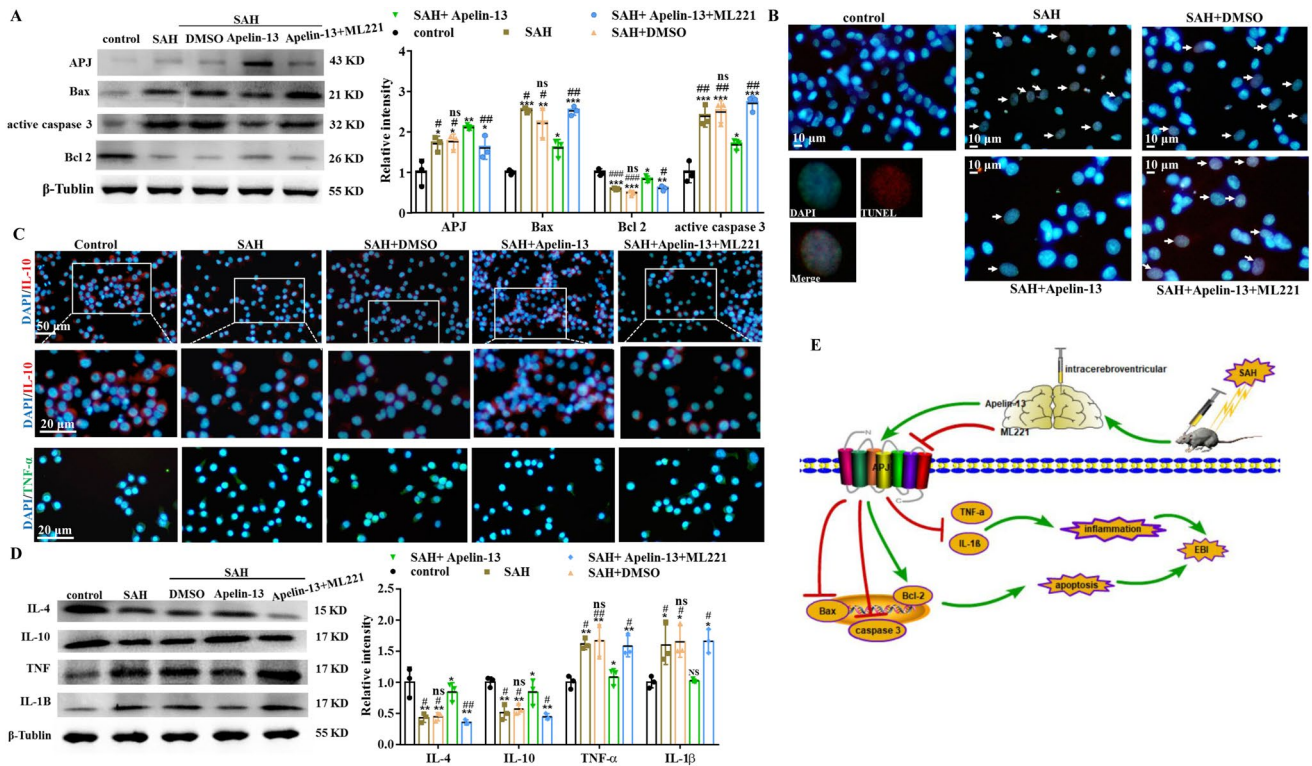


Fig. 5 Apelin-13 inhibited apoptosis and inflammation in an APJ-dependent manner after SAH in vitro. **A** Western blot indicated the protein levels of APJ, Bax, Bcl-2, and active caspase 3 in each group. **B** Detection of apoptosis by TUNEL staining. Scale bar was 10 μm. **C** The content of TNF-α and IL-10 was detected by IF. Scale bar was 50 μm for upper and 20 μm for down. **D** Western blot indicated the protein levels of IL-4, IL-10, TNF-α, and IL-1β in BV-2 cells. **E** Schematic diagram of the possible mechanism of apelin-13/APJ system on EBI after SAH. The present study illustrates that, following establishment of SAH, the pro-apoptosis protein of Bax and

active caspase 3 were significantly increased, while the anti-apoptosis protein of Bcl-2 was suppressed. The excessive cell apoptosis lead to the brain injury. On the contrary, exogenous apelin-13 suppresses the expression of pro-apoptosis proteins, and promoted Bcl-2 expression, which attenuates the EBI through inhibiting apoptosis. In addition, the neuroprotective role of apelin-13 can be blocked by ML221 via inhibiting expression of APJ receptor. *Mean $P < 0.05$ vs control, NS mean $P > 0.05$ vs control, #Mean $P < 0.05$ vs Apelin-13, ns mean $P > 0.05$ vs SAH. **Mean $P < 0.01$, ***Mean $P < 0.001$

that ML221 did not indicate significant effect on progesterone production or proliferation in bovine ovarian cells unless cells were stimulated with recombinant apelin-13 [21]. Therefore, apelin-13 protect against brain damage after SAH in an APJ dependent manner. APJ mediates apelin-13 to protect against brain injury after SAH, and antagonism of ML221 to APJ may be depend on apelin-13.

Apelin-13 can regulate the apoptotic signaling pathway and thus reduce the number of apoptotic neurons in the cortex during SAH, which may be another mechanism of apelin-13 to protect brain tissue. Apoptosis is a kind of program cell death pathway and play a crucial role in EBI induced by SAH. Pro-apoptotic Bcl-2 family members take part in and activate caspase-9 to trigger further the downstream effector caspases, including caspase-3, caspase-6, and caspase-7 through the intrinsic apoptotic pathway [22]. As is well known, cell apoptosis is enhanced after SAH, where Bax and caspase 3 were up-regulated, while Bcl-2, an apoptotic inhibitor, was down-regulated.

Importantly, previous study reported that apelin shows strong anti-apoptosis effect and ameliorates EBI after SAH in rats [19]. Another study showed that apelin-13 pre-treatment can diminish memory impairment by inhibiting apoptosis in an Alzheimer's disease [23, 24]. In our study, the cell apoptosis was reflected by apoptosis-related markers, the expression levels of Bax and active caspase 3 were significantly elevated while Bcl-2 was suppressed in rats after SAH, but apelin-13 partially revised these effect. Furthermore, ML221 could partially reduce the effect of apelin-13 on apoptosis-related marker. Thus, apelin-13 could protect against cell apoptosis after SAH via intervening the expression of Bax, Bcl-2 and active caspase 3 in an APJ dependent manner. In addition, TUNEL, FJB and Nissl staining also indicated that apelin-13 decreased the cell death and attenuated SAH-induced EBI in an APJ dependent manner. Taken together, these results revealed that apelin-13 exhibits neuroprotective role against SAH-induced EBI through attenuating apoptosis.

We also realize there were some limitations in our work. To be first, the present study only explored the neuroprotective effects of apelin-13 in the early stages of SAH to male rats. Thus, its long-term neuroprotective roles and sex difference require further investigation in SAH-induced brain damage and neurological deficits. Secondly, our study demonstrated that apelin-13 can only partially attenuate neuronal apoptosis dependent on APJ expression, implying other molecular mechanisms involved which need further investigation.

Conclusion

In summary, our current study confirms that apelin-13 exhibits the neuroprotective role to attenuate EBI following SAH, which is mediated by inhibiting neuronal apoptosis in an APJ dependent manner following SAH in rats. These findings confirmed that apelin-13 could be developed as a novel drug for treatment of SAH. Apelin-13/APJ system as an endogenous signaling pathway played a crucial role during SAH and should be explored further in the future.

Supplementary Information The online version contains supplementary material available at <https://doi.org/10.1007/s11033-021-07028-y>.

Acknowledgements The authors thank Mr. Zhi Li for his linguistic assistance during the preparation of this manuscript.

Author contributions All authors had full access to all the data in the study and take responsibility for the integrity of the data and the accuracy of the data analysis. Study concept and design: GC, ZW and HS. Acquisition of data: XS, and GY. Analysis and interpretation of data: BL, CC, DC, and JW. Drafting manuscript: XS, and GY. Administrative, technical, and material support: HL, and XL. Study supervision: GC, ZW and HS.

Funding This work was supported by the National Natural Science Foundation of China (Nos. 81873741 & 82071297).

Declarations

Conflict of interests The authors declare that they have no conflict of interests.

Ethical approval All animal experiments were approved by the Institutional Animal Care Committee of Soochow University and were performed in accordance with the guidelines of the National Institutes of Health.

References

- Macdonald RL, Schweizer TA (2017) Spontaneous subarachnoid haemorrhage. *Lancet* 389:655–666. [https://doi.org/10.1016/S0140-6736\(16\)30668-7](https://doi.org/10.1016/S0140-6736(16)30668-7)
- Balbi M, Vega MJ, Lourdopoulos A et al (2019) Long-term impairment of neurovascular coupling following experimental subarachnoid hemorrhage. *J Cereb Blood Flow Metab.* <https://doi.org/10.1177/0271678X19863021>
- Suzuki H (2019) Inflammation: a good research target to improve outcomes of poor-grade subarachnoid hemorrhage. *Transl Stroke Res* 10:597–600. <https://doi.org/10.1007/s12975-019-00713-y>
- Mejdoubi M, Schertz M, Zanolta S et al (2018) Transoceanic management and treatment of aneurysmal subarachnoid hemorrhage: a 10-year experience. *Stroke* 49:127–132. <https://doi.org/10.1161/STROKEAHA.117.017436>
- Xie YK, Zhou X, Yuan HT et al (2019) Resveratrol reduces brain injury after subarachnoid hemorrhage by inhibiting oxidative stress and endoplasmic reticulum stress. *Neural Regen Res* 14:1734–1742. <https://doi.org/10.4103/1673-5374.257529>
- Conzen C, Becker K, Albanna W et al (2019) The acute phase of experimental subarachnoid hemorrhage: intracranial pressure dynamics and their effect on cerebral blood flow and autoregulation. *Transl Stroke Res* 10:566–582. <https://doi.org/10.1007/s12975-018-0674-3>
- Naraoka M, Fumoto T, Li Y et al (2019) The role of intracranial pressure and subarachnoid blood clots in early brain injury after experimental subarachnoid hemorrhage in rats. *World Neurosurg* 129:e63–e72. <https://doi.org/10.1016/j.wneu.2019.05.009>
- Kleinz MJ, Davenport AP (2005) Emerging roles of apelin in biology and medicine. *Pharmacol Ther* 107:198–211. <https://doi.org/10.1016/j.pharmthera.2005.04.001>
- Bao H, Yang X, Huang Y et al (2016) The neuroprotective effect of apelin-13 in a mouse model of intracerebral hemorrhage. *Neurosci Lett* 628:219–224. <https://doi.org/10.1016/j.neulet.2016.06.046>
- Duan J, Cui J, Yang Z et al (2019) Neuroprotective effect of Apelin 13 on ischemic stroke by activating AMPK/GSK-3beta/Nrf2 signaling. *J Neuroinflamm* 16:24. <https://doi.org/10.1186/s12974-019-1406-7>
- Tian X, Sun L, Feng D et al (2017) HMGB1 promotes neurovascular remodeling via rage in the late phase of subarachnoid hemorrhage. *Brain Res* 1670:135–145. <https://doi.org/10.1016/j.brainres.2017.06.001>
- Yang Y, Zhang X, Cui H et al (2014) Apelin-13 protects the brain against ischemia/reperfusion injury through activating PI3K/Akt and ERK1/2 signaling pathways. *Neurosci Lett* 568:44–49. <https://doi.org/10.1016/j.neulet.2014.03.037>
- Xiong Q, He W, Wang H et al (2017) Effect of the spinal apelin-APJ system on the pathogenesis of chronic constriction injury-induced neuropathic pain in rats. *Mol Med Rep* 16:1223–1231. <https://doi.org/10.3892/mmr.2017.6734>
- Zhang Z, Wu Y, Yuan S et al (2018) Glutathione peroxidase 4 participates in secondary brain injury through mediating ferroptosis in a rat model of intracerebral hemorrhage. *Brain Res* 1701:112–125. <https://doi.org/10.1016/j.brainres.2018.09.012>
- Li P, Li X, Deng P et al (2020) Activation of adenosine A3 receptor reduces early brain injury by alleviating neuroinflammation after subarachnoid hemorrhage in elderly rats. *Aging* 13:694–713. <https://doi.org/10.18632/aging.202178>
- Angelopoulou E, Paudel YN, Bougea A et al (2021) Impact of the apelin/APJ axis in the pathogenesis of Parkinson's disease with therapeutic potential. *J Neurosci Res.* <https://doi.org/10.1002/jnr.24895>
- O'Donnell LA, Agrawal A, Sabnekar P et al (2007) Apelin, an endogenous neuronal peptide, protects hippocampal neurons against excitotoxic injury. *J Neurochem* 102:1905–1917. <https://doi.org/10.1111/j.1471-4159.2007.04645.x>
- Xu W, Gao L, Li T et al (2018) Apelin-13 alleviates early brain injury after subarachnoid hemorrhage via suppression of endoplasmic reticulum stress-mediated apoptosis and blood-brain barrier disruption: possible involvement of ATF6/CHOP pathway. *Neuroscience* 388:284–296. <https://doi.org/10.1016/j.neuroscience.2018.07.023>

19. Liu Y, Zhang T, Wang Y et al (2019) Apelin-13 attenuates early brain injury following subarachnoid hemorrhage via suppressing neuronal apoptosis through the GLP-1R/PI3K/Akt signaling. *Biochem Biophys Res Commun* 513:105–111. <https://doi.org/10.1016/j.bbrc.2019.03.151>
 20. Xu W, Li T, Gao L et al (2019) Apelin-13/APJ system attenuates early brain injury via suppression of endoplasmic reticulum stress-associated TXNIP/NLRP3 inflammasome activation and oxidative stress in a AMPK-dependent manner after subarachnoid hemorrhage in rats. *J Neuroinflamm* 16:247. <https://doi.org/10.1186/s12974-019-1620-3>
 21. Roche J, Rame C, Reverchon M et al (2017) Apelin (APLN) regulates progesterone secretion and oocyte maturation in bovine ovarian cells. *Reproduction* 153:589–603. <https://doi.org/10.1530/REP-16-0677>
 22. Datta A, Sarmah D, Mounica L et al (2020) Cell death pathways in ischemic stroke and targeted pharmacotherapy. *Transl Stroke Res*. <https://doi.org/10.1007/s12975-020-00806-z>
 23. Aminyavari S, Zahmatkesh M, Farahmandfar M et al (2019) Protective role of Apelin-13 on amyloid beta25-35-induced memory deficit; involvement of autophagy and apoptosis process. *Prog Neuropsychopharmacol Biol Psychiatry* 89:322–334. <https://doi.org/10.1016/j.pnpbp.2018.10.005>
 24. Zou Y, Wang B, Fu W et al (2016) Apelin-13 protects PC12 cells from corticosterone-induced apoptosis through PI3K and ERKs activation. *Neurochem Res* 41:1635–1644. <https://doi.org/10.1007/s11064-016-1878-0>
- Publisher's Note** Springer Nature remains neutral with regard to jurisdictional claims in published maps and institutional affiliations.